

Photocycloaddition of 9,10-Dichloroanthracene to 2,5-Dimethyl-2,4-hexadiene. The Singlet Pathway for [4 + 2]-Adduct Formation in Benzene

Jack Saltiel,* Reza Dabestani,[†] Donald F. Sears, Jr., William M. McGowan, and Edwin F. Hilinski*

Contribution from the Department of Chemistry, Florida State University, Tallahassee, Florida 32306-3006, and Oak Ridge National Laboratory, Oak Ridge, Tennessee 37831-6100

Received March 9, 1995[®]

Abstract: Irradiation of 9,10-dichloroanthracene (DCA) in the presence of 2,5-dimethyl-2,4-hexadiene (DMHD) in benzene at 25 °C gives a single adduct (Ad) corresponding to [4 + 2] addition of DMHD to the 9,10 positions of DCA. Quantum yields for Ad formation are reported as a function of [DMHD], [DCA], and methyl iodide concentration, [MeI]. Fluorescence quantum yields and lifetimes of DCA and (DCA/DMHD) singlet exciplex as a function of [MeI] are also reported. Transient absorption measurements reveal the time evolution of excited DCA singlet, ¹DCA*, and triplet, ³DCA*, states and of the (DCA/DMHD) singlet exciplex, ¹(DCA·DMHD)*. They show that the dominant decay path from ¹(DCA·DMHD)* gives ³DCA*. Quenching of ¹DCA* and exciplex fluorescence and transient absorption by MeI are observed. The dependence of Ad quantum yields on [DMHD] and the strict proportionality between product quantum yields and exciplex fluorescence quantum yields at different [MeI] establish a singlet mechanism for adduct formation. Assuming that Ad is a primary photoproduct, the results are consistent with Yang's proposal of stepwise collapse of polar exciplexes to seemingly forbidden cycloadducts. A singlet biradical could be the intermediate, but intersystem crossing of the singlet exciplex to a triplet biradical as the initial step cannot be ruled out. The loss of DCA is enhanced at very high [DMHD] but oxygen quenching experiments show that this enhancement does not involve formation of the triplet biradical by addition of ³DCA* to DMHD.

Singlet exciplex formation between arenes and 1,3-dienes was first suggested by Hammond and co-workers to account for 1,3-diene quenching of arene fluorescence.¹ The formation of photoadducts from the interaction of electronically excited arenes, notably anthracenes, with 1,3-dienes was reported by the groups of Yang² and Kaupp³ soon thereafter. Observations of exciplex fluorescence in specific cases^{2d,f,4} suggested them as viable intermediates for adduct formation, but compelling evidence for such a mechanism was first obtained by Caldwell

and co-workers for phenanthrene/olefin systems for which exciplex specific quenchers were shown to quench exciplex fluorescence and adduct formation with identical efficiencies.⁵ Photoaddition of anthracenes to 1,3-dienes gives [4 + 4], [4 + 2], and [2 + 2] cycloadducts,^{2,3} but the preferred cycloaddition mode is very sensitive to substituents on either reactant and to the solvent.^{2,3} The Woodward–Hoffmann rules⁶ and other molecular orbital approaches⁷ predict that photochemically concerted suprafacial cycloadditions involving 4*n* electrons are allowed whereas those involving 4*n* + 2 electrons are forbidden. To account for the observation of forbidden [4 + 2] adducts in anthracene/1,3-diene systems Yang proposed^{2c,e} a competition between concerted and stepwise collapse of singlet exciplexes, the latter process leading to [4 + 2] addition. Kaupp, on the other hand, has postulated direct competing stepwise biradical pathways to allowed and forbidden photoadducts. Since some

* Address correspondence to this author at Florida State University.

[†] Oak Ridge National Laboratory.

[®] Abstract published in *Advance ACS Abstracts*, August 15, 1995.

(1) (a) Stephenson, L. M.; Whitten, D. G.; Vesley, G. F.; Hammond, G. S. *J. Am. Chem. Soc.* **1966**, *88*, 3665, 3893. (b) Stephenson, L. M.; Hammond, G. S. *Pure Appl. Chem.* **1968**, *16*, 125. (c) Stephenson, L. M.; Hammond, G. S. *Angew. Chem., Int. Ed. Engl.* **1969**, *8*, 261. (d) Evans, T. R. *J. Am. Chem. Soc.* **1971**, *93*, 2081. (e) Labianca, D. A.; Taylor, G. N.; Hammond, G. S. *J. Am. Chem. Soc.* **1972**, *94*, 3679. (f) Taylor, G. N.; Hammond, G. S. *J. Am. Chem. Soc.* **1972**, *94*, 3684, 3687.

(2) (a) Yang, N. C.; Libman, J. *J. Am. Chem. Soc.* **1972**, *94*, 1405. (b) Yang, N. C.; Libman, J.; Barrett, L.; Hui, M. H.; Loesch, R. L. *J. Am. Chem. Soc.* **1972**, *94*, 1406. (c) Yang, N. C.; Neywick, C.; Srinivasachar, K. *Tetrahedron Lett.* **1975**, 4313. (d) Yang, N. C.; Shold, D. M.; McVey, J. K. *J. Am. Chem. Soc.* **1975**, *97*, 5004. (e) Yang, N. C.; Srinivasachar, K.; Kim, B.; Libman, J. *J. Am. Chem. Soc.* **1975**, *97*, 5006. (f) Yang, N. C.; Yates, R. L.; Masnovi, J.; Shold, D. M.; Chiang, W. *Pure Appl. Chem.* **1979**, *51*, 173. (g) Yang, N. C.; Shold, D. M. *J. Chem. Soc., Chem. Commun.* **1978**, 978. (h) Yang, N. C.; Masnovi, J.; Chiang, W. *J. Am. Chem. Soc.* **1979**, *101*, 6465. (i) Yang, N. C.; Shou, H.; Wang, T.; Masnovi, J. *J. Am. Chem. Soc.* **1980**, *102*, 6652. Also see: Caldwell, R. A. *J. Am. Chem. Soc.* **1980**, *102*, 4004.

(3) (a) Kaupp, G. *Angew. Chem., Int. Ed. Engl.* **1972**, *11*, 718. Also see: Kaupp, G. *Angew. Chem., Int. Ed. Engl.* **1972**, *11*, 313. (b) Kaupp, G.; Dyllick-Brenzinger, R.; Zimmerman, I. *Angew. Chem., Int. Ed. Engl.* **1975**, *18*, 491. (c) Kaupp, G. *Leibigs Ann. Chem.* **1977**, 254. (d) Kaupp, G.; Grüter, H.-W. *Angew. Chem., Int. Ed. Engl.* **1979**, *18*, 881. (e) Kaupp, G.; Grüter, H.-W. *Chem. Ber.* **1980**, *113*, 1458. (f) Kaupp, G.; Schmitt, D. *Chem. Ber.* **1981**, *114*, 1567. (g) Kaupp, G.; Grüter, H. W.; Teufel, E. *Chem. Ber.* **1983**, *116*, 630. (h) Kaupp, G.; Teufel, E. *Chem. Ber.* **1980**, *113*, 3669.

(4) (a) Taylor, G. N. *Chem. Phys. Lett.* **1971**, *10*, 355. (b) Saltiel, J.; Townsend, D. E. *J. Am. Chem. Soc.* **1973**, *95*, 6140. (c) Saltiel, J.; Townsend, D. E.; Watson, B. D.; Shannon, P. *J. Am. Chem. Soc.* **1975**, *97*, 5688.

(5) (a) Caldwell, R. A.; Smith, L. *J. Am. Chem. Soc.* **1974**, *96*, 2994. (b) Caldwell, R. A.; Creed, D.; DeMarco, D. C.; Melton, L. A.; Ohta, H.; Wine, P. H. *J. Am. Chem. Soc.* **1980**, *102*, 2369. (c) Caldwell, R. A.; Creed, D. *Acc. Chem. Res.* **1980**, *13*, 45 and references therein. (d) Majima, T.; Pac, C.; Shakurai, H. *Bull. Chem. Soc. Jpn.* **1978**, *51*, 1811. (e) Pac, C.; Sakurai, H. *Chem. Lett.* **1976**, 1067. (f) Itoh, M.; Takita, N.; Matsumoto, M. *J. Am. Chem. Soc.* **1979**, *101*, 7363.

(6) Woodward, R. B.; Hoffmann, R. *The Conservation of Orbital Symmetry*; Academic Press: New York, 1970.

(7) (a) Zimmerman, H. E. *Acc. Chem. Res.* **1971**, *4*, 272. (b) Dougherty, R. C. *J. Am. Chem. Soc.* **1971**, *93*, 7187. (c) Michl, J. *Mol. Photochem.* **1974**, *4*, 243, 257, 287.

[4 + 4] adducts thermally rearrange to [4 + 2] adducts at moderate temperatures the latter can also form as secondary products.³

It has also been recognized that the change in the order of energy levels that leads to exoergic electron transfer in polar exciplexes may open an allowed concerted pathway to [4_s + 2_s] adducts.⁸ A key difference between [4_s + 2_s] reactions of relatively nonpolar exciplexes that are dominated by the locally excited state of one of the partners (semipolar cycloadditions) and of polar exciplexes that can be represented as contact radical-ion pairs (polar cycloadditions) is the relative symmetry of their singly occupied molecular orbitals (SOMO's). SOMO's of an exciplex (or reaction complex) undergoing a semipolar [4_s + 2_s] cycloaddition are of different symmetry leading to the usual correlation with a highly excited product.⁶ In contrast, SOMO's of an exciplex undergoing a polar [4_s + 2_s] cycloaddition are of the same symmetry allowing, *in addition*, direct correlation with ground state product.⁸ Whether this alternative pathway is controlling in specific systems is not clear, as we are aware of no experimental evidence demonstrating its existence.

Alternatively, addition of arene triplets to 1,3-dienes could give triplet biradicals whose collapse to adducts could account for [4 + 2] products. Early precedents for the triplet pathway include cycloadditions of acenaphthylene⁹ and phenanthrene¹⁰ to olefins and the nonregiospecific addition of the 1,2-bond of 1,3-pentadienes across the 9,10 positions of benz[*a*]anthracene triplets to yield [4 + 2] adducts, exclusively.¹¹ The results of a quantitative study of the photocycloaddition of anthracene (A) to *trans,trans*-2,4-hexadiene (HD) led to less clear-cut conclusions.¹² Although allowed [4 + 4] adducts have excited singlet state precursors and the forbidden [4 + 2] adduct is the major product from triplet anthracene addition to the diene, about 8% of singlet exciplexes give the forbidden [4 + 2] adduct as well.¹²

We demonstrated earlier that the photocycloaddition of 9,10-dichloroanthracene (DCA) to 1,3-cyclohexadiene (CHD)^{2c} gives allowed [2 + 2] and [4 + 4] adducts via singlet exciplex pathways in both benzene and acetonitrile.¹³ In benzene the [4 + 2] adduct is observed only in trace amounts.¹³ We were puzzled, therefore, by the striking substituent dependence on the mode of addition exhibited by 2,5-dimethyl-2,4-hexadiene (DMHD).^{2a,e} DMHD in benzene gives mainly [4 + 4] addition with anthracene, [4 + 4] and [4 + 2] addition with 9-fluoroanthracene, and only [4 + 2] addition with DCA or 9,10-dicyanoanthracene.^{2a,e} The interest in the DCA/DMHD system is enhanced, because being the first arene/1,3-diene system for which exciplex fluorescence was reported,^{4b} it is well-characterized spectroscopically,^{2d,4c} and because in contrast to DCA/CHD, it gives exclusively the forbidden [4 + 2] adduct. The work described in this paper concerns the mechanism of this cycloaddition.

Results

Photochemical Observations. A. Preparative. Preparative-scale irradiations (404-nm) of DCA, 0.034 M, and DMHD,

(8) (a) Epitotis, N. D.; Yates, R. L. *J. Org. Chem.* **1974**, *39*, 3150. (b) Epitotis, N. D. *Angew. Chem., Int. Ed. Engl.* **1974**, *13*, 751-780.

(9) Feree, W. I., Jr.; Plummer, B. F.; Schloman, W. W., Jr. *J. Am. Chem. Soc.* **1974**, *96*, 7741 and other papers in this series.

(10) (a) Caldwell, R. A. *J. Am. Chem. Soc.* **1973**, *95*, 1960. (b) Caldwell, R. A.; Creed, D. *J. Am. Chem. Soc.* **1977**, *99*, 8360. (c) Caldwell, R. A.; Creed, D.; Maw, T.-S. *J. Am. Chem. Soc.* **1979**, *101*, 1293.

(11) Saltiel, J.; Townsend, D. E.; Metts, L. L.; Wrighton, M.; Mueller, W.; Rosanske, R. C. *J. Chem. Soc., Chem. Commun.* **1978**, 588.

(12) Saltiel, J.; Dabestani, R.; Schanze, K. S.; Trojan, D.; Townsend, D. E.; Goedken, V. L. *J. Am. Chem. Soc.* **1986**, *108*, 2674.

(13) Smothers, W. K.; Meyer, M. C.; Saltiel, J. *J. Am. Chem. Soc.* **1983**, *105*, 545.

Table 1. Effect of DMHD on DCA Loss in Benzene at 25 °C^a

[DMHD], M	10 ³ φ _{-DCA} ^b	10 ³ φ _{-DCA}
0.051 ₉	0.52(2)	
0.069 ₂	0.64(2)	0.61(6)
0.083 ₀	0.70(3)	
0.086 ₅	0.70(2)	
0.110 ₇	0.80(2)	0.85(3)
0.138 ₃	0.84(3)	0.93 ^d
0.138 ₃	0.87 ^e	
0.138 ₃	0.70 ^{e,f}	
0.166 ₀		1.02(3)
0.208	1.01(4)	1.12(4)
0.277		1.11 ^d
0.41 ₅	1.31(4)	1.42(5)
0.69 ₂	1.47(3)	1.60(11)
1.10 ₇		1.92(10)
1.38 ₃	2.25(10)	1.89 ^d
1.38 ₃	1.91 ^{e,f} 1.84 ^{e,g}	
1.38 ₃	1.26 ^{e,h}	

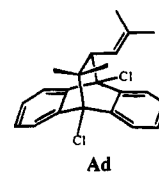
^a Average deviations from up to six independent determinations are given in parentheses. ^b [DCA]₀ = 6.48–6.67 × 10⁻⁴ M. ^c [DCA]₀ = 2.02 × 10⁻³ M. ^d From Table 2. ^e Based on φ_{-DCA} = 2.25 × 10⁻³ at 1.38₃ M [DMHD]. ^f Air-saturated solution. ^g Air-bubbled solution. ^h O₂-bubbled solution.

Table 2. MeI Effect on DCA Loss Quantum Yields in the Presence of DMHD in Benzene at 25.0 °C^a

[MeI], M	[DMHD], M	10 ³ φ _{-DCA} ^b
0	1.38 ₃	1.89(5) ^c
0.32	1.38 ₃	1.55(2)
0.64	1.38 ₃	1.25
0.96	1.38 ₃	1.12(2)
1.28	1.38 ₃	1.01(2)
1.60	1.38 ₃	0.91(1)
1.93	1.38 ₃	0.81
1.93	1.38 ₃	0.82 ^d
0	0.277	1.11 ^{d,e}
0	0.138 ₃	0.93 ^{d,e}
0.32	0.138 ₃	0.71 ^d

^a [DCA] = 2.04 × 10⁻³ M. ^b Values in parentheses are deviations from the mean in the last significant digit employing two different actinometers, see text. ^c Extrapolated value based on the following seven entries. ^d DCA loss by UV and Ad yield by ¹H NMR. ^e These values used in actinometry, see text.

1.06 M, in the absence and presence of methyl iodide, [MeI] = 1.36 M, in Ar-purged benzene as solvent were carried out as previously reported.¹³ Analysis by ¹H NMR confirmed Yang's report of the formation of a single product, Ad,^{2a,d} in benzene



and the identical result was obtained in the presence of MeI: isolated yields of 58 and 73%, respectively, mp 133.5–135.0 °C, mixed mp 133.0–134.0 °C; ¹H NMR (270 MHz, CDCl₃) δ 0.65 (s, 3 H, bridge methyl), 0.86 (s, 3 H, bridge methyl), 1.59 (s, 3 H, allylic methyl), 1.69 (s, 3 H, allylic methyl), 2.73 (d, *J* = 11 Hz, 1 H, allylic), 4.42 (d, *J* = 11 Hz, 1 H, vinyl), 7.26 (m, 4 H), 7.64 (m, 1 H), 7.73 (m, 3 H).

B. Photoreaction Quantum Yields. DCA loss quantum yields, φ_{-DCA}, were determined as a function of [DMHD] (Table 1) and as a function of [MeI] at constant [DMHD] in benzene (Table 2). These were generally based on UV analyses except in four selected cases (last four entries in Table 2) for which the yield of Ad was directly measured also by ¹H NMR based independently on the bridgehead methyl proton signals and on

Table 3. MeI Effect on DCA Fluorescence^a

[MeI], M	(<i>I</i> ⁰ / <i>I</i>) _{deg}	(<i>I</i> ⁰ / <i>I</i>) _{air}
0.	1.00	1.26(1)
0.32	1.06(1)	1.30(1)
0.64	1.09(1)	1.32(1)
0.96	1.14(1)	1.42(1)
1.28	1.20(1)	1.46(1)
1.60	1.28(1)	1.52(2)

^aRelative intensity at 414 nm, [DCA] = 5.32×10^{-5} M in benzene; numbers in parentheses give deviations in the last significant digit from the mean of duplicate determinations.

Table 4. MeI Effect on Fluorescence Lifetimes^a

[MeI], M	[DMHD] = 0 τ_{fm} , ns	[DMHD] = 0.69 ₂ M τ_r , ns
0.	9.50(30); 7.26(10)	6.30(29); 5.50(10)
0.32	8.89(10); 6.92(10)	
0.64	8.58(10); 6.74(10)	4.68(26); 4.30(20)
1.60		3.44(23); 3.16(20)

^aBenzene solutions with [DCA] = 6.5×10^{-5} M; λ_{exc} = 360 nm, $\lambda_{em} \geq 380$ nm, and $\lambda_{em} \geq 510$ nm numbers in parentheses give standard deviations in the last significant digit(s) shown; the two sets of entries are for degassed and air-saturated solutions, respectively.

the aromatic protons of Ad. The range of % DCA losses by UV, 11.0–17.5% for the four solutions was in very good agreement with the range of % Ad yields by ¹H NMR, 9.7–17.4%. Especially good agreement was obtained for the highest two conversions (14.3% vs 14.4% and 17.5% vs 17.4%) leading to the conclusion that $\phi_{-DCA} = \phi_{Ad}$. [DCA] was measured by UV spectroscopy immediately following the irradiation period and at different times during a dark period of several days at 25 °C or several hours at ~50 °C for [DCA] = 2.04×10^{-3} M and [DMHD] = 0.69₂ M. No DCA loss was observed during the dark periods.

Irradiations were conducted in a Moses merry-go-round apparatus¹⁴ at 25.0 ± 0.1 °C with 366-nm excitation. The benzophenone-sensitized isomerization of *trans*-stilbene was used for actinometry¹⁵ and conversions to *cis*-stilbene were corrected for zero-time *cis* content and back reaction.¹⁶ In view of the relatively low cycloaddition quantum yields, several actinometer solutions were irradiated in series with the DCA/DMHD samples as previously reported.¹³ The results in Table 1 give average ϕ_{-DCA} values from several independent experiments employing widely different ranges of % DCA loss (from a low of 5–17% to a high of 23–72%). They include ϕ_{-DCA} values in the presence of oxygen.

Spectroscopic Measurements. A. Steady State. Quenching of DCA fluorescence by MeI was determined in benzene both in the absence (Table 3) and in the presence of DMHD (Table 4). Excitation was at 360 nm at 25.0 °C. Anomalously high quenching results were obtained using 340-nm excitation apparently due to significant absorption by MeI at the high concentrations employed. The results are for degassed solutions except in the absence of DMHD for which relative emission yields in the presence of air are also reported (Table 3). Relative DCA fluorescence yields were based on relative intensity of the 0–0 band (~414 nm) and relative exciplex fluorescence yields were based on fluorescence intensity at 500 nm.

B. Transient Fluorescence Observations. The effect of MeI on DCA fluorescence decay rate constants was determined

in the absence and in the presence of DMHD, 0.69₂ M. Air-saturated solutions of DCA, 6.4×10^{-5} M, in benzene were employed. Excitation was at 360 nm and decay was monitored for $\lambda_{em} \geq 380$ nm and for $\lambda_{em} \geq 510$. Lifetimes are shown in Table 4. Results obtained for $\lambda_{em} \geq 510$ nm, for which the exciplex fluorescence in the presence of diene makes a much larger contribution, were, within experimental uncertainty, identical to those for $\lambda_{em} \geq 380$ nm. The average values for the two emission wavelengths are shown in Table 4.

C. Transient Absorption Spectra. Transient absorption spectra were recorded at –40, –30, –20, –10, 0, 10, 20, 30, 50, 70, 100, 300, 500, 1500, 4500, 9500, and 19500 ps after excitation for each of the following samples in benzene at 22 °C: (a) 2.04×10^{-3} M DCA; (b) 2.04×10^{-3} M DCA and 1.93 M MeI; (c) 2.04×10^{-5} M DCA and 0.69₂ M DMHD; and (d) 2.04×10^{-3} M DCA, 1.93 M MeI, and 0.69₂ M DMHD. Representative spectra are shown in Figure 1. Each spectrum is an average of 400 laser shots with average pulse energies in the 145–173 μ J range. Spectra shown in Figure 1 are normalized to a pulse energy of 170 μ J. Common features of the spectra under these different conditions are the prompt appearance, within the time duration of the 25-ps 355-nm excitation pulse, of a broad absorption with a maximum near 600 nm and the onset of a second absorption band at ~450 nm. The main absorption band at ~600 nm undergoes a band shape change that is probably due to vibrational relaxation within the first 30–70 ps following the excitation pulse. This early transient spectrum is assigned to $S_n \leftarrow S_1$ DCA transitions. As it decays in the nanosecond time scale it is replaced by a $T_n \leftarrow T_1$ absorption band with λ_{max} at 435–440 nm that persists for times longer than 20 ns after excitation. The $T_n \leftarrow T_1$ absorption in benzene was previously reported to have λ_{max} at 435 nm¹⁷ in agreement with our observations. The sharp decrease in detectable probe light intensity and the large DCA fluorescence in our baseline prevent measurement of spectra at wavelengths lower than ~435 nm under our conditions. Approximate rate constants derived from the spectral evolutions in Figure 1 are not reported because they are somewhat larger than those obtained from the fluorescence measurements suggesting incomplete elimination of air from the solutions.

Discussion

The determination of whether singlet or triplet excited DCA is the precursor of Ad is based, in large part, on the external heavy-atom effect (HAE). Interaction with molecules containing heavy atoms enhances spin-orbital coupling in other molecules. The external HAE facilitates both radiative and nonradiative singlet-triplet transitions.¹⁸ Photochemical consequences of enhanced $S_1 \rightarrow T_1$ probability are attenuation of quantum yields of singlet-derived products and enhancement of quantum yields of triplet-derived products. At very high heavy atom concentrations quantum yields of triplet-derived products also decrease due to significant, though less pronounced, induced $T_1 \rightarrow S_0$ intersystem crossing. These photochemical effects were first demonstrated when the external HAE was used in the elucidation of the mechanisms of acenaphthylene photodimerization¹⁹ and cross-adduct formation.⁹ For anthracene/1,3-diene systems the effect of including MeI as cosolvent is an increase of the relative

(17) Kemp, T. J.; Roberts, J. P. *Trans. Faraday Soc.* **1969**, *65*, 725.

(14) Moses, F. G.; Liu, R. S. H.; Monroe, B. M. *Mol. Photochem.* **1969**, *1*, 245.

(15) (a) Hammond, H. A.; DeMeyer, D. E.; Williams, J. L. R. *J. Am. Chem. Soc.* **1969**, *91*, 5180. (b) Valentine, D., Jr.; Hammond, G. S. *J. Am. Chem. Soc.* **1972**, *94*, 3449.

(16) Saltiel, J.; Marinari, A.; Chang, D. W.-L.; Mitchener, J. C.; Megarity, E. D. *J. Am. Chem. Soc.* **1979**, *101*, 2982.

(18) (a) Lower, S. K.; El-Sayed, M. A. *Chem. Rev.* **1966**, *66*, 199. (b) McGlynn, S. P.; Azumi, T.; Kinoshita, M. *Molecular Spectroscopy of the Triplet State*; Prentice-Hall: Englewood Cliffs, NJ, 1969. (c) Birks, J. B. *Photophysics of Aromatic Molecules*; Wiley-Interscience: New York, 1970. (d) Wilkinson, F. *Organic Molecular Photophysics*; Birks, J. B., Ed.; Wiley-Interscience: New York, 1975; Vol. 2, p 95. (e) Haselbach, E.; Pilloud, D.; Suppan, P. *EPA Newsl.* **1988**, *No. 33*, 41.

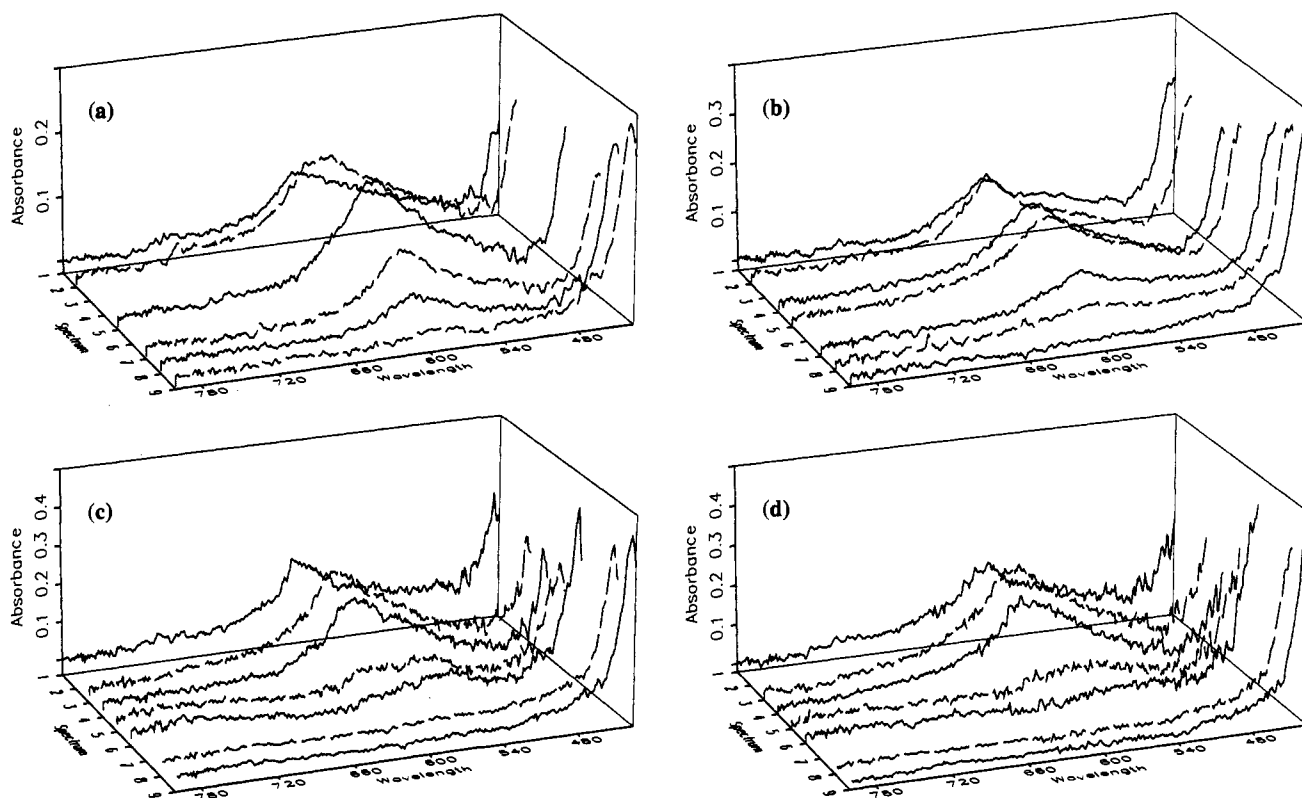


Figure 1. Transient absorption spectra recorded at selected times after 355-nm excitation of 2.04×10^{-3} M DCA in benzene: alone (a) and in the presence of 1.93 M MeI (b), 0.692 M DMHD (c), and 1.93 M MeI together with 0.692 M DMHD (d). Delay times in increasing order from back to front, time (spectrum number), are the following: 10 (1), 30 (2), 50 (3), 100 (4), 500 (5), 1500 (6), 4500 (7), 9500 (8), and 19500 (9) ps. Absorbances in spectra 1–6 in (c) and (d) are multiplied by 2.

yield of [4 + 2] adducts.^{2f,12} The more quantitative study of the external HAE on the photochemistry of the A/HD system is consistent with quenching of [4 + 4] singlet adducts and promotion of [4 + 2] adduct via the triplet pathway due to enhanced $S_1 \rightarrow T_1$ intersystem crossing in A.¹² As will be shown below, our results for the DCA/DMHD system lead to the surprising conclusion that Ad, the only observed photoadduct, derives formally from a forbidden [4 + 2] singlet state pathway.

Ad Quantum Yields with No MeI. In anticipation of our conclusion that Ad forms directly from the addition of $^1\text{DCA}^*$ to DMHD, the interpretation of the quantum yields in Table 1 is based on Scheme 1. With the exception of the exciplex fluorescence step, Scheme 1 is identical to the scheme employed to account for the photoadducts in the DCA/CHD system.¹³ However, though identical kinetic schemes apply, only the forbidden [4 + 2] mode appears to be active with DMHD, whereas only allowed [4 + 4] and [2 + 2] modes are active with CHD.¹³

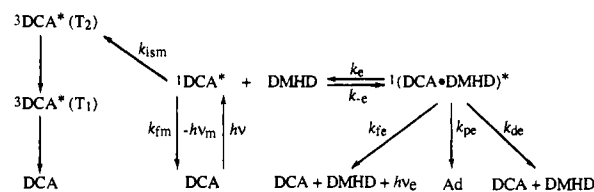
Application of the steady-state approximations for all excited species in Scheme 1 predicts

$$(\phi_{-\text{DCA}})^{-1} = (\phi_{\text{Ad}})^{-1} = (\phi_{\text{Ad}}^{\text{lim}})^{-1} \left(1 + \frac{1}{pk_e\tau_m^0[\text{DMHD}]} \right) \quad (1)$$

where $\tau_m^0 = (k_{\text{fm}} + k_{\text{ism}})^{-1}$ is the $^1\text{DCA}^*$ lifetime in the absence of quenchers, $p = (k_{\text{de}} + k_{\text{fe}} + k_{\text{pe}})/(k_{-e} + k_{\text{de}} + k_{\text{fe}} + k_{\text{pe}})$ is the fraction of exciplexes that do not regenerate $^1\text{DCA}^*$, and

(19) (a) Cowan, D. O.; Drisko, R. L. *Tetrahedron Lett.* **1967**, 1255. (b) Cowan, D. O.; Drisko, R. L. *J. Am. Chem. Soc.* **1967**, 89, 3068; **1970**, 92, 6281, 6282. (c) Cowan, D. O.; Kozjar, J. C. *J. Am. Chem. Soc.* **1974**, 96, 1229; **1975**, 97, 249. (d) Cowan, D. O.; Drisko, R. L. *Elements of Organic Photochemistry*; Plenum Press: New York, 1976.

Scheme 1



$\phi_{\text{Ad}}^{\text{lim}} = k_{\text{pe}}\tau_e^0$, where $\tau_e^0 = (k_{\text{de}} + k_{\text{fe}} + k_{\text{pe}})^{-1}$ is the exciplex lifetime, is the limiting quantum yield for Ad formation obtained by extrapolation to infinite [DMHD].¹³

With the exception of the product-forming step, the rate constants of all other processes are known from spectroscopic observations.^{4c} As the concentration of DMHD is increased in benzene at 23.5 °C, the blue emission of $^1\text{DCA}^*$ diminishes and is replaced by a weaker green exciplex emission, $\lambda_{\text{max}} = 485$ nm. An isoemissive point at ~ 515 nm for [DMHD] ≤ 2.76 M shows that $^1\text{DCA}^*$ and $^1(\text{DCA}\cdot\text{DMHD})^*$ have a stoichiometric relationship. The Stern–Volmer plot for $^1\text{DCA}^*$ fluorescence quenching by DMHD yielded $pk_e\tau_m^0 = 14.0 \text{ M}^{-1}$.^{4c} Inclusion of the two additional points measured in this work doubles the [DMHD] range, extending it to 1.383 M, without significantly affecting the Stern–Volmer constant, $pk_e\tau_m^0 = 13.9 \pm 0.2 \text{ M}^{-1}$. That the decays of monomer and exciplex are coupled due to rapid equilibrium between them was established by the observation of identical nanosecond time scale fluorescence lifetimes for monomer and exciplex that decrease only slightly with increasing [DMHD] ($\sim 35\%$ τ decrease at [DMHD] = 2.76 M!).^{4c}

It follows that for the yields in Table 1 to adhere to eq 1 the plot of ϕ_{Ad}^{-1} vs [DMHD]⁻¹ should be linear with intercept to slope ratio $i/s = pk_e\tau_m^0 = 13.9 \text{ M}^{-1}$. That this condition is obeyed rather well for [DMHD] ≤ 0.138 M, especially for the

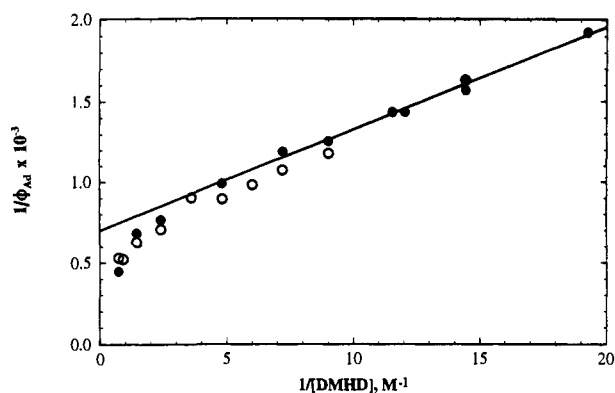


Figure 2. The dependence of ϕ_{Ad} on $[DMHD]$ in benzene for low (●) and high (○) $[DCA]$.

quantum yields for low $[DCA]_0$, is shown in Figure 2. The top six quantum yields in column 2 of Table 1 are consistent with $\phi_{Ad}^{lim} = (1.27 \pm 0.06) \times 10^{-3}$ from the intercept and $i/s = pk_e\tau_m^0 = 14.0 \pm 0.9 \text{ M}^{-1}$ in good agreement with the spectroscopic value. However, at higher $[DMHD]$, results of at least ten independent experiments summarized in Table 1 consistently show higher than expected product quantum yields. Since the quantum yields are based primarily on the loss of DCA rather than of Ad formation (cf., however, the last four entries in Table 2), the trend to higher apparent ϕ_{Ad} 's at higher $[DMHD]$'s may have reflected formation of $[4 + 4]$ adduct as a minor, as yet undetected, product. A precedent exists in the *A/trans,trans*-2,4-hexadiene system where thermal addition of A to the trans double bond of the $[4 + 4]$ adduct increases the observed loss of A and, if not taken into account, leads to erroneously large ϕ_{Ad} 's.^{3h,12} Such a thermal reaction could account for the reported failure to observe the $[4 + 4]$ adduct in the DCA·DMHD system by ¹H NMR within a 1% detection limit.^{2c} This possibility was ruled out in our work by UV measurements that reveal no further DCA loss even on heating irradiated solutions in the dark for prolonged periods following irradiation.

By analogy with observations on the *A/trans,trans*-2,4-hexadiene¹² and on the DCA/1,3-cyclohexadiene¹³ systems, we had initially expected that, as most ¹DCA* is intercepted by DMHD, participation of ³DCA* in the cycloaddition would not be likely at the highest $[DMHD]$ employed. Surprisingly, the transient absorption measurements in Figure 1c throw a very different light on potential involvement of triplets. The prompt appearance of the 600-nm band of ¹DCA* is again observed, and at somewhat longer times a shoulder near 550 nm and enhanced absorption from 650 to 795 nm also develop. These differences in absorption, evident at 0.5 and 1.5 ns in Figure 1c relative to the same time range of Figure 1a, most likely reflect formation of ¹(DCA·DMHD)* as the dominant species at 0.69₂ M DMHD in equilibrium with ¹DCA*. Furthermore, at longer times, they show that the presence of the diene leads to a 1.6-fold enhancement in the yield of ³DCA*. The intersystem crossing yield, $\phi_{ism} = 0.29$, of DCA in toluene²⁰ agrees well with values of 0.29–0.36 based on fluorescence quantum yields measured in benzene.^{4c,21–23} It follows that in the presence of the diene ϕ_{is} increases to roughly 0.46–0.58 indicating that intersystem crossing is the major decay pathway of the exciplex (about 91% of ¹DCA* is diverted to exciplex in the presence of 0.69₂ M DMHD^{4c}). Furthermore, ³DCA* in eq 2 must form directly in T₁ because, if T₂ were initially

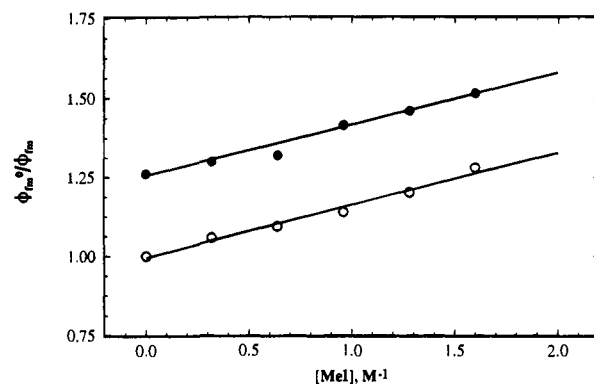
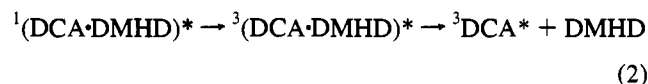


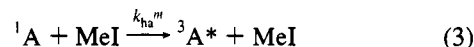
Figure 3. The quenching of ¹DCA* fluorescence by MeI in benzene for degassed (○) and air-saturated (●) solutions.

formed, its efficient quenching by DMHD^{24,25} would suppress T₁ formation.



Consequently, participation of DCA triplets in cycloaddition at the high $[DMHD]$ range may account for the downward deviation of the points in Figure 2. As will be shown below, this interesting possibility is ruled out by oxygen quenching experiments.

The External HAE on ¹DCA* Fluorescence. In view of the very efficient quenching of anthracene fluorescence by MeI that we observed earlier, $k_{ha}^m = 5.5 \times 10^9 \text{ M}^{-1} \text{ s}^{-1}$ in benzene



at 23 °C,¹² the quenching of ¹DCA* fluorescence by MeI, Table 3, seems at first glance anomalously inefficient. Stern–Volmer plots of the data in Table 3, shown in Figure 3, generate two parallel lines showing that MeI and O₂ quenching of ¹DCA* are strictly additive events (eq 6). Data for degassed solutions give $s = k_{ha}^m\tau_m^0 = 0.163 \pm 0.010 \text{ M}^{-1}$ with fixed $i = 1.00$ and data for air-saturated solutions, omitting the point for $[MeI] =$



$$\phi_{fm}^0/\phi_{fm} = 1 + k_q\tau_m^0[O_2] + k_{ha}^m\tau_m^0[MeI] \quad (6)$$

0.64 M, give $s_{ox} = k_{ha}^m\tau_m^0 = 0.162 \pm 0.004 \text{ M}^{-1}$ and $k_q\tau_m^0[O_2] = 0.256 \pm 0.005 \text{ M}^{-1}$ from the slope and intercept, respectively. The displacement of the two lines in Figure 3 from each other agrees with previous measurements of the effect of O₂ on ¹DCA* fluorescence.^{4c,13} The fact that $s = s_{ox}$ shows that no cooperative quenching of ¹DCA* by MeI and O₂ occurs in the concentration ranges employed.^{4c,13,26} Thus, participation of ¹(DCA·MeI)* and ³(DCA·O₂)* exciplexes with significant lifetimes need not be proposed to account for these observations.

Use of $k_{ha}^m\tau_m^0 = 0.163 \text{ M}^{-1}$ and $\tau_m^0 = 9.8 \text{ ns}$ (average from refs 4c, 21, and 26) gives $k_{ha}^m = 1.6_6 \times 10^7 \text{ M}^{-1} \text{ s}^{-1}$ for ¹DCA* which is 330 times smaller than the corresponding rate constant for ¹A*. Plots of fluorescence decay rate constants

(24) Saltiel, J.; Townsend, D. E.; Sykes, H. *J. Am. Chem. Soc.* **1983**, *105*, 2530.

(25) Bohne, C.; Kennedy, S. R.; Boch, R.; Negri, F.; Orlandi, G.; Siebrand, W.; Scaiano, J. C. *J. Phys. Chem.* **1991**, *95*, 10300.

(26) Charlton, J. L.; Townsend, D. E.; Watson, B. D.; Shannon, P.; Kowalewska, N.; Saltiel, J. *J. Am. Chem. Soc.* **1977**, *99*, 5992.

(27) Ware, W. R. *J. Phys. Chem.* **1962**, *66*, 455.

(20) Darmayan, A. P. *Chem. Phys. Lett.* **1984**, *110*, 89.

(21) Bowen, E. J.; Sahu, J. *J. Phys. Chem.* **1959**, *63*, 4.

(22) Ware, W. R.; Baldwin, B. A. *J. Chem. Phys.* **1964**, *40*, 1703.

(23) Dawson, W. R.; Windsor, M. W. *J. Phys. Chem.* **1968**, *72*, 3251.

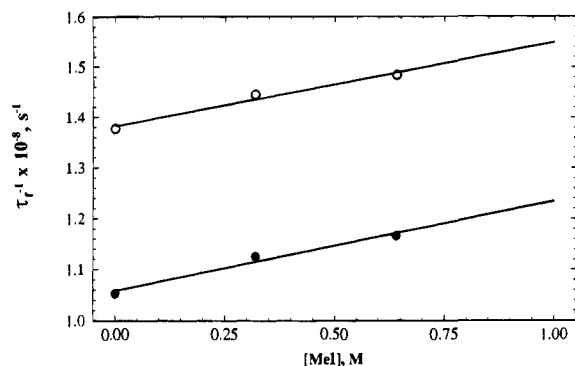


Figure 4. The effect of MeI on fluorescence decay rate constants of DCA in degassed (●) and in air-saturated (○) benzene.

from Table 4 as a function of [MeI], Figure 4, give $k_{ha}^m = (1.77 \pm 0.28) \times 10^7$ and $(1.67 \pm 0.26) \times 10^7 \text{ M}^{-1} \text{ s}^{-1}$ for degassed and air-saturated solutions, respectively, well within experimental uncertainty of the more precise results from the steady state observations. Normally, chlorine substitution would be expected to enhance k_{ha}^m up to the limiting diffusion-controlled value. It is well established that the external HAE enhances spin-orbit coupling pathways already present in a molecule.¹⁸ Since DCA singlet-triplet transitions experience a larger internal HAE due to the chlorines, a correspondingly larger external HAE on DCA is expected. However, in contrast to the $T_1 \rightarrow S_0$ transition whose overall rate is enhanced 32 times in DCA²⁸ relative to A,²⁹ and the $S_1 \rightarrow T_1$ transition in naphthalene which is similarly enhanced upon chlorine substitution, the internal HAE seems to produce no analogous effect in the $S_1 \rightarrow T_1$ transition of DCA. In fact, in contrast to naphthalene, both τ_f^0 , 4.2 and 9.8 ns in benzene for A and DCA, respectively, and ϕ_f , 0.27 and 0.64, in the same order, are enhanced instead of diminished upon introduction of the meso chlorine substituents. This anomaly is well understood having been traced to the energy required to form a T_2 state, nearly isoenergetic with S_1 , as the initial intersystem crossing process from S_1 in anthracenes.^{24,25,30-33} The $S_1 \rightarrow T_2$ process is exoergic in A. It is rendered endoergic in DCA because meso halogen substitution lowers the energy of S_1 more than that of T_2 . Endoergic intersystem crossing from S_1 to T_2 more than cancels any benefits from enhanced spin-orbit coupling (evident in the preexponential factor for the process) and, overall, a reduced rate constant for the process results. The considerations that give the appearance of an inverse internal HAE have a more profound effect on the external HAE for the $S_1 \rightarrow T$ process in DCA. It is likely that the quenching interaction which very probably gives T_2 initially in eq 3 gives T_1 directly in eq 4. That this is an attractive possibility is indicated by the recent demonstration that $O_2(^3\Sigma)$ quenching of $^1A^*$ gives T_2 of A and no $O_2(^1\Delta)$, while $O_2(^3\Sigma)$ quenching of $^1DCA^*$, eq 5, gives T_1 of DCA and $O_2(^1\Delta)$.³³ It appears that

(28) Saltiel, J.; Marchand, G. R.; Kirkor-Kaminska, E.; Smothers, W. K.; Mueller, W. B.; Charlton, J. L. *J. Am. Chem. Soc.* **1984**, *106*, 3144.

(29) Saltiel, J.; Marchand, G. R.; Dabestani, R.; Pecha, J. M. *Chem. Phys. Lett.* **1983**, *100*, 219.

(30) (a) Kellogg, R. E. *J. Chem. Phys.* **1966**, *44*, 411. (b) Bennett, R. G.; McCartin, P. J. *J. Chem. Phys.* **1966**, *44*, 1969. (c) Lim, E. C.; Laposa, J. D.; Yu, J. M. H. *J. Mol. Spectrosc.* **1966**, *19*, 412.

(31) See, especially: (a) Gillispie, G. D.; Lim, E. C. *J. Chem. Phys.* **1976**, *65*, 2022. (b) Gillispie, G. D.; Lim, E. C. *Chem. Phys. Lett.* **1979**, *63*, 355.

(32) (a) Hunter, T. F.; Wyatt, R. F. *Chem. Phys. Lett.* **1970**, *6*, 221. (b) Widman, R. P.; Huber, J. R. *J. Phys. Chem.* **1972**, *76*, 1524. (c) Kearvell, A.; Wilkinson, F. *Transitions Non Radiat. Mol., Reun. Soc. Chim. Phys., 20th, 1969* **1970**, 125.

(33) Wilkinson, F.; McGarvey, D. J.; Olea, A. F. *J. Am. Chem. Soc.* **1993**, *115*, 12144.

Table 5. MeI Effect on DCA and (DCA·DMHD) Exciplex Fluorescence^a

[MeI], M	[DMHD] = 0.69 ₂ M		[DMHD] = 1.38 ₃ M	
	(ϕ_{fm}^0/ϕ_{fm})	(ϕ_{fe}^0/ϕ_{fe})	(ϕ_{fm}^0/ϕ_{fm})	(ϕ_{fe}^0/ϕ_{fe})
0	10.6 ^b	1.10 ₃	20.1	1.05 ₂
0.32			24.2	1.27
0.40	12.1	1.36		
0.64	12.7	1.49	26.9	1.45
0.80	13.8	1.63		
0.96	14.3	1.74	29.0	1.64
1.20	14.6	1.78		
1.44	15.6	2.10		
1.60			36.0	2.07
1.76	16.1	2.28		

^a DCA and (DCA·DMHD) exciplex emissions monitored at 414 and 500 nm, respectively; [DCA] = 6.30×10^{-5} and 5.32×10^{-5} M in benzene for [DMHD] = 0.69₂ and 1.38₃ M, respectively. ^b Calculated based on $pk_c\tau_m^0 = 13.9 \text{ M}^{-1}$, see text.

the encounters in eqs 4 and 5 do not produce sufficiently long-lived complexes to allow enhancement of the activated $S_1 \rightarrow T_2$ process to contribute significantly in either quenching event. Further support for this interpretation is provided by the observation that rate constants for quenching of the fluorescence of a series of aromatic hydrocarbons by *n*-propyl iodide in benzene decrease exponentially with the increase in the S_1-T_n energy gap, where *n* designates the triplet state populated in the quenching event.³⁴ The fluorescence of aromatic hydrocarbons, such as anthracene, that have accessible higher triplet states is quenched much more efficiently than the fluorescence of those that do not.³⁴

The proportionality between k_{ism} and k_{ha}^m values that was observed recently with 1,4-dibromobenzene as quencher,^{18e} should hold only when the same triplet state is formed initially in the two intersystem crossing events. Our conclusion that k_{ism} and k_{ha}^m are associated with $^3DCA^*(T_2)$ and $^3DCA^*(T_1)$ formation, respectively, leads us to expect that DCA should deviate strongly from the published^{18e} correlation.

Based on the fluorescence quenching observations, it can be shown that for the two extremes of none or all of the MeI quenching events leading to $^3DCA^*$ a 31% decrease or a 42% enhancement of $T_1 \rightarrow T_n$ absorbance, respectively, is expected at 1.93 M MeI. The observed enhancement of 30% (19.5-ns spectrum in panels (a) and (b) of Figure 1) is well within experimental uncertainty of the enhancement predicted by eq 4.

The External HAE's on Monomer and Exciplex Fluorescence. As previously discussed, Scheme 1, $^1DCA^*$ and $^1(DCA\cdot DMHD)^*$ fluorescences are observed when DMHD is present. These emissions are both quenched by MeI, Table 5. Since monomer and exciplex decays are strongly coupled due to rapid equilibration of the two species,^{4c} quenching of either was expected to be reflected in diminished fluorescence intensity of the other. Indeed, slopes of Stern-Volmer plots of $^1DCA^*$ fluorescence quenching by MeI are strongly enhanced in the presence of DMHD (Figure 5), $s = 4.2 \pm 0.3$ and $9.9 \pm 0.6 \text{ M}^{-1}$ for [DMHD] = 0.69₂ and 1.38₃ M, respectively. In principle, two cooperative quenching events involving DMHD and MeI could account for these results. The long lifetime of the DCA·DMHD singlet exciplex virtually ensures a MeI quenching step such as eq 7 and the high DMHD concentrations employed may allow eq 8 to come into play although the presence of $^1(DCA\cdot MeI)^*$ is not revealed when a relatively small oxygen concentration is present as a second quencher, (Figure 4). Thus, diminished $^1(DCA\cdot DMHD)^*$ fluorescence in the presence of MeI probably reflects direct quenching of the

(34) Dresskamp, Von H.; Koch, E.; Zander, M. *Ber. Bunsenges. Phys. Chem.* **1974**, *78*, 1328-1334.

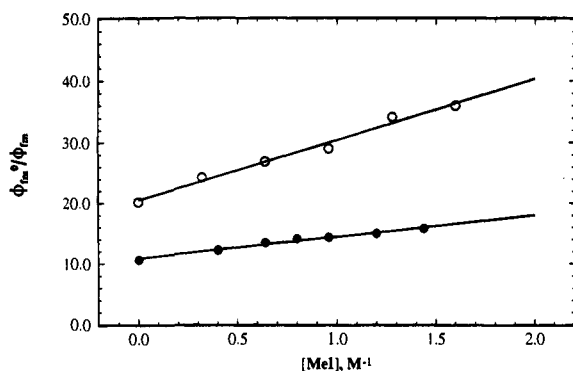
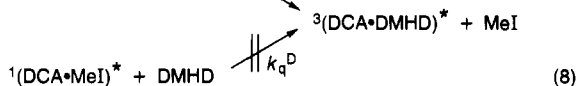


Figure 5. The quenching of $^1\text{DCA}^*$ fluorescence by MeI in degassed benzene in the presence of $[\text{DMHD}] = 0.69_2$ (●) and 1.38_3 M (○).



exciplex via eq 7 and/or lower exciplex formation efficiency via eq 8. Support for this conclusion is provided by the transient absorption spectra in Figure 1. Comparison of panels (c) and (d) shows that decay of $^1\text{DCA}^*$ to an equilibrium mixture with $^1(\text{DCA}\cdot\text{DMHD})^*$, the dominant species, is followed by even more efficient $^3\text{DCA}^*$ formation in the presence of MeI. The 1.7-fold enhancement in $^3\text{DCA}^*$ absorbance indicates an effective $^3\text{DCA}^*$ formation quantum yield in the 0.49–0.61 range. This is consistent with eq 7 as it is likely that, if it exists at all, dissociation to $^3\text{DCA}^*$ and DMHD is the primary fate of the triplet exciplex.

Neglecting for the moment the trapping of a $^1(\text{DCA}\cdot\text{MeI})^*$ exciplex or encounter complex by DMHD gives

$$\phi_{fm}^0/\phi_{fm}^{D,M} = 1 + p^M k_e \tau_m^0 [\text{DMHD}] + k_{ha}^m \tau_m^0 [\text{MeI}] \quad (9)$$

for monomer fluorescence quenching where $\phi_{fm}^{D,M}$ is the $^1\text{DCA}^*$ fluorescence quantum yield in the presence of diene and methyl iodide, and

$$p^M = \frac{1 + k_{ha}^e \tau_e^0 [\text{MeI}]}{1 + k_{-e} \tau_e^0 + k_{ha}^e \tau_e^0 [\text{MeI}]} \quad (10)$$

Based on this assumption, the enhanced slopes in Figure 5 relative to Figure 3 reflect the increase in p^M with increasing [MeI] and the difference in [DMHD]. The corresponding expression for the quenching of $^1(\text{DCA}\cdot\text{DMHD})^*$ exciplex fluorescence is

$$\frac{\phi_{fe}^0}{\phi_{fe}} = \left(\frac{1 + p^M k_e \tau_m^0 [\text{DMHD}] + k_{ha}^m \tau_m^0 [\text{MeI}]}{p^M k_e \tau_m^0 [\text{DMHD}]} \right) (1 + k_{ha}^e \tau_m^0 [\text{MeI}]) \quad (11)$$

Combining eqs 9 and 11 gives

$$\left(\frac{\phi_{fe}^0}{\phi_{fe}} \right) \left(1 - \frac{\phi_{fm}^{D,M} \phi_{fm}^0}{\phi_{fm}^0 \phi_{fm}^M} \right) = 1 + k_{ha}^e \tau_e^0 [\text{MeI}] \quad (12)$$

where ϕ_{fm}^M is the $^1\text{DCA}^*$ fluorescence quantum yield in the presence of MeI and the ϕ_{fe}^0/ϕ_{fe} ratios, Table 5, are based on $k_{fe} \tau_e^0 = 0.0622$, the previously determined^{4c} limiting exciplex

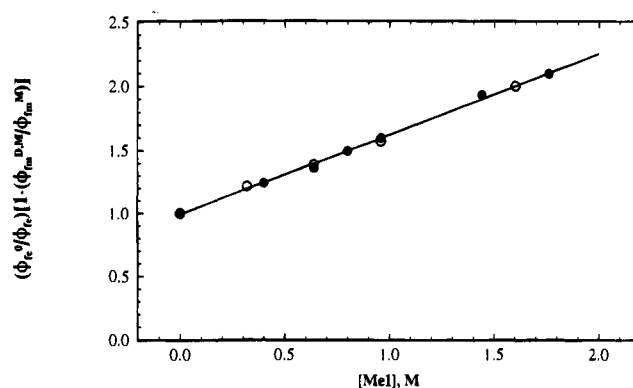


Figure 6. Relative emission quantum yields plotted according to eq 12 for $[\text{DMHD}] = 0.69_2$ (●) and 1.38_3 M (○).

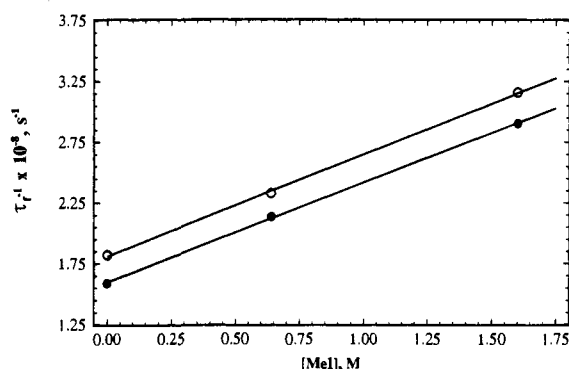


Figure 7. The effect of MeI on monomer/excimer fluorescence decay rate constants in the presence of $[\text{DMHD}] = 0.69_2$ M for degassed (●) and air-saturated (○) benzene solutions.

fluorescence quantum yield at high [DMHD] in the absence of MeI. The data in Table 5 adhere closely to eq 12 (Figure 6), giving $k_{ha}^e \tau_e^0 = 0.64 \pm 0.02$ and 0.62 ± 0.02 for $[\text{DMHD}] = 0.69_2$ and 1.38_3 M, respectively. The near identity of the lines in Figure 6, independent of [DMHD], shows that the contribution of eq 8 to fluorescence quenching, if any, is negligible. The average of the slopes and $\tau_e^0 = 7.4$ ns from ref 4c give $k_{ha}^e = (8.5 \pm 0.4) \times 10^7 \text{ M}^{-1} \text{ s}^{-1}$, which is about five times larger than k_{ha}^m . A somewhat larger k_{ha}^e value would result if the shorter τ_e^0 value from Table 4 were employed. An independent rough estimate of k_{ha}^e can be based on the fluorescence lifetimes in Table 4 in the presence of [DMHD]. Since fluorescence decay rate constants are, within experimental uncertainty, independent of the range of monitored λ_{em} , $^1\text{DCA}^*$ and $^1(\text{DCA}\cdot\text{DMHD})^*$ appear to exist in rapid equilibrium at $[\text{DMHD}] = 0.69_2$ M. For the special case of complete monomer/excimer equilibration the observed decay rate constant is a weighted average of the decay rates of monomer and exciplex. Grouping the [MeI] terms gives

$$\tau_f^{-1} = \frac{(\tau_m^0)^{-1} + k_q^m [\text{O}_2] + K_e [\text{DMHD}] \{ (\tau_e^0)^{-1} + k_q^e [\text{O}_2] \}}{1 + K_e [\text{DMHD}]} + \frac{(k_{ha}^m + K_e [\text{DMHD}] k_{ha}^e) [\text{MeI}]}{1 + K_e [\text{DMHD}]} \quad (13)$$

The slopes of the plots of the decay rate constants in Figure 7 and the known K_e and k_{ha}^m values (see ref 4c and above, respectively) give $k_{ha}^e = (8.7 \pm 0.2) \times 10^7$ and $(8.9 \pm 0.3) \times 10^7 \text{ M}^{-1} \text{ s}^{-1}$, for degassed and air-saturated solutions, respectively, in very good agreement with the value determined from the steady-state observations.

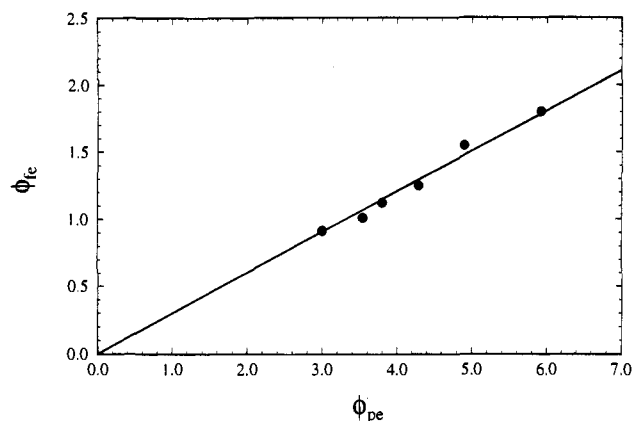


Figure 8. The relationship of ϕ_{Ad} and ϕ_{fe} as a function of [MeI] in benzene.

Correlation of Product and Exciplex Fluorescence Quantum Yields. Based on Scheme 1 and the quenching steps in eqs 4 and 7, the expression for product quantum yields,

$$\phi_{pe} = \frac{P^M k_e \tau_m^0 [\text{DMHD}]}{1 + P^M k_e \tau_m^0 [\text{DMHD}] + k_{ha}^m \tau_m^0 [\text{MeI}]} \frac{k_{pe} \tau_e^0}{1 + k_{ha}^e \tau_e^0 [\text{MeI}]} \quad (14)$$

is analogous to that for ϕ_{fe} (compare eq 11 with eq 14). It follows that, if the exciplex were the sole source of the product, ϕ_{pe} and ϕ_{fe} should be strictly proportional to each other as one varies [MeI] at constant [DMHD]

$$\phi_{pe} = \frac{k_{pe}}{k_{fe}} \phi_{fe} \quad (15)$$

The quantum yields for [DMHD] = 1.38₃ M from Tables 2 and 5 adhere nicely to eq 15 (Figure 8). The slope of the line forced through the origin yields $(k_{pe}/k_{fe}) = 0.030 \pm 0.002$. Though the parallel behavior of exciplex fluorescence and Ad formation yields points strongly to common singlet precursors for the two processes, it does not preclude the possibility that intersystem crossing from the exciplex to ³DCA* precedes the formation of Ad. The spectra in Figure 1d show that, as expected, MeI interactions with ¹(DCA·DMHD)* lead to a substantial increase in the yield of ³DCA*. MeI enhanced triplet yields in other systems produce corresponding increases in the quantum yields of triplet derived products, except at very high [MeI] for which arene triplet lifetimes are sufficiently shortened to cause an overall quenching of triplet product formation.^{12,17,18} Since the opposite result obtains in our system, we conclude that, in contrast to the other cases cited above, ³DCA* is not an intermediate in the main pathway that leads to the forbidden [4 + 2] adduct. Although we favor the singlet exciplex as the precursor of the adduct, our results do not establish it as an obligatory precursor in this case. To the extent that ¹DCA* and ¹(DCA·DMHD)* exist in facile equilibrium even in the presence of MeI, the two species are kinetically indistinguishable. It follows that the transition state leading to Ad may differ from geometries favored by the singlet exciplex. Such a transition state could be attained as a parallel process to exciplex formation and/or as a parallel process to exciplex dissociation. Since a stepwise mechanism is likely to apply we attach little significance to this distinction.

Based on our favored mechanism, ¹(DCA·CHD)* and ¹(DCA·DMHD)* exciplexes utilize allowed¹³ and forbidden pericyclic pathways to adducts, respectively. Since DMHD is

a much better electron donor than CHD,¹³ the charge distribution in ¹(DCA·DMHD)* must be much closer to the contact radical-ion pair extreme than that in ¹(DCA·CHD)*. The more favorable energetics for electron transfer in ¹(DCA·DMHD)* are reflected in the formation of separated radical-ions and complete suppression of the cycloaddition pathway in acetonitrile,³⁵ whereas, in the same solvent, cycloadditions via allowed pathways remain the dominant reaction modes of ¹(DCA·CHD)*.¹³ We are led to the conclusion that, provided that Ad is a primary photoproduct, the most attractive explanation for the sharp contrast in the cycloaddition pathways utilized by these two DCA·diene singlet exciplexes in benzene is Yang's proposal of concerted collapse of nonpolar exciplexes to allowed [2 + 2] and [4 + 4] adducts, but stepwise collapse of polar exciplexes to seemingly forbidden [4 + 2] adducts.^{2c,d} To retain a concerted pathway to [4 + 2] adducts, it would be necessary to adopt the postulate⁸ of a relaxation of the Woodward–Hoffmann rules for polar exciplexes.

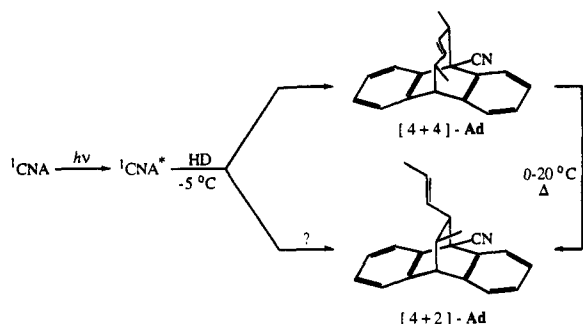
The efficient exciplex decay channel to ³DCA* that is revealed by the transient absorption measurements may also be a consequence of increased charge separation in the exciplex. Electron transfer in the ¹DCA*/DMHD encounter complex has been estimated to be exothermic by 7.6 kcal/mol in acetonitrile,¹³ and the experimental enthalpy change (ΔH) for exciplex formation in methylcyclohexane is -5.7 ± 0.1 kcal/mol.^{2d} Thus the singlet exciplex is probably best represented as a contact radical-ion pair in benzene, ¹(DCA⁻·DMHD⁺)*. Enhanced intersystem crossing in the back electron transfer step probably reflects the diminished energy gap between the charge transfer stabilized exciplex and ³DCA*(T₁).³⁶ No such stabilization is expected in the DCA/CHD singlet exciplex.¹³ The curvature in the plot in Figure 2 suggests that DCA triplets produced from the exciplex lead to adduct at high [DMHD]. To test this possibility, a separate experiment was performed in which relative DCA losses were measured in degassed and air-saturated benzene at low (0.138₃ M) and high (1.38₃ M) [DMHD] (Table 1). Due to the much longer ³DCA* lifetime,²⁸ it was anticipated that the presence of O₂ should completely eliminate any possible ³DCA* participation in adduct formation. The proposed explanation for the curvature in Figure 2 would require a much more pronounced O₂ quenching effect at high [DMHD]. Contrary to this expectation, observed ratios of ϕ_{-DCA} for degassed and air-saturated solutions at low and high [DMHD] are 1.24 and 1.18, respectively. In order to avoid the possibility of O₂ depletion in the irradiated solutions, the high [DMHD] experiment was repeated with continuous air and O₂ bubbling throughout the irradiation period. Ratios of ϕ_{-DCA} for degassed to air-bubbled and to O₂-bubbled solutions are 1.22 and 1.79, respectively (Table 1). These small ratios are consistent with the expected quenching of ¹DCA* and the somewhat shorter lived ¹(DCA·DMHD)* exciplex (expected ratios based on eq 10 and 14 with O₂ terms substituted for the MeI terms are 1.22 for air-bubbled and 2.16 for O₂-bubbled solutions). Thus, any significant direct ³DCA* addition to DMHD is ruled out. However, it is likely that in systems with more reactive arene triplets efficient intersystem crossing from singlet exciplex to arene triplet may not only lead to diminished yields of adducts from concerted [2 + 2] and [4 + 4] reactions but may give enhanced yields of triplet derived adducts.

As a referee has pointed out, formation of an allowed [4 + 4] adduct that thermally rearranges to the observed [4 + 2] adduct under our reaction conditions could account for our results. Kaupp et al. have shown that [4 + 4] adducts of 1,3-

(35) Smothers, W. K.; Schanze, K. S.; Saltiel, J. *J. Am. Chem. Soc.* **1979**, *101*, 1985.

(36) We thank Dr. S. Farid for this suggestion.

Scheme 2



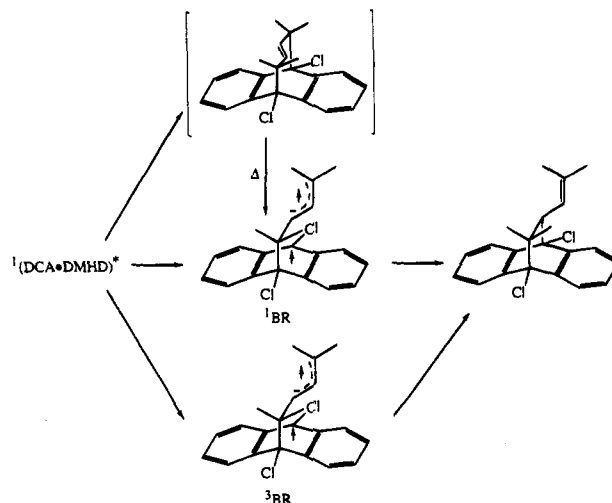
dienes at the 9,10-positions of anthracenes (including DCA) are of variable thermal stability and, depending on the anthracene/diene partners, rearrange to the [4 + 2] adducts at temperatures ranging from 0 to >150 °C.^{3e-g} Especially relevant is the photoaddition of 9-cyanoanthracene (CNA) to *trans,trans*-2,4-hexadiene (HD) in benzene, (Scheme 2). The only adduct obtained upon room temperature irradiation is [4 + 2]-Ad.^{2b} However, low-temperature irradiation and workup yield a 3:2 mixture of [4 + 4]-Ad to [4 + 2]-Ad (¹H NMR), and on warming in the dark to 20 °C the major [4 + 4]-Ad is converted nearly quantitatively to the [4 + 2]-Ad.^{3g} If this reaction sequence operated in our system, it would eliminate the puzzle of accounting for the formation of a formally forbidden photoproduct. Formation of other photoproducts that are not observed due to thermal reversion to the starting materials (see for instance a report of such an occurrence for the DCA/1,3-cyclopentadiene system^{3d}) would contribute in the overall quenching constant (i.e., in the magnitude of *p* in eq 1) but would in no way affect our conclusions concerning the formation of Ad.

Assuming that Ad is a primary photoproduct, a mechanism involving collapse of ¹(DCA·DMHD)* to a singlet biradical (¹BR) as its precursor is a viable possibility. Transient absorption spectra observed following picosecond-pulse excitation of 9-cyanoanthracene in neat DMHD have been assigned by Mataga and co-workers to such an intermediate.³⁷ The assignment was based in part on the absorption spectrum ($\lambda_{\max} \approx 520$ nm) of the 9-cyano-10-hydranthryl radical.³⁷ Absorption in approximately the same region has also been assigned to a 9-nitro-10-hydranthryl radical.³⁸ In view of the unexplained enhancement of DCA loss at the highest [DMHD]'s used in our study (Figure 1), we are concerned about the validity of the interpretation of spectroscopic observations at even higher [DMHD]. The intermediate assigned to ¹BR by Mataga is fully formed within 100 ps following pulse excitation and decays with the same lifetime (0.57 ns) as the lifetime of the exciplex. The much longer exciplex lifetime in our system precludes observation of such a short-lived intermediate in our transient absorption spectra.

The high efficiency of intersystem crossing from ¹(DCA·DMHD)* raises the possibility that a competing intersystem crossing channel directly to a triplet biradical may better explain the stepwise collapse to Ad. For this unprecedented mechanism to be viable, MeI must preferentially enhance the intersystem crossing channel leading to ³DCA*. This possibility would be consistent with our earlier conclusion that MeI opens a direct decay path from ¹DCA* to ³DCA*(T₁) instead of enhancing the normal intersystem crossing pathway to ³DCA*(T₂), if the triplet biradical pathway of the exciplex shown in Scheme 2 were subject to a significant activation energy.

(37) Okada, T.; Kida, K.; Mataga, N. *Chem. Phys. Lett.* **1982**, *88*, 157-160.

Scheme 3



Alternatively, the singlet exciplex, being predominantly a contact radical-ion pair, may undergo intersystem crossing to give a triplet contact radical-ion pair³⁹ prior to ³DCA* and triplet biradical, ³BR, formation. Absorption from ³BR is not observed



in Figure 1 (the 19.5-ns spectra in panels (c) and (d) show only ³DCA* absorption). However, if it were involved, its formation is likely to be inefficient in view of the low ϕ_{Ad} values. Its absorbance in the visible spectral region (~520 nm)^{37,38} is expected to be weak and would not be observable within the experimental noise of our spectra. We plan to pursue the question of ¹BR vs ³BR intermediates in future experiments with analogue systems.

Three possible mechanisms for the formation of Ad are summarized in Scheme 3. A fourth would involve concerted Ad formation directly from the exciplex.⁸ If the [4 + 4] adduct is the primary photoproduct we favor a concerted pathway for its formation and a biradical pathway for its rearrangement. There seems to be no good reason why a singlet biradical would collapse to the highly strained [4 + 4] adduct, as proposed by Kaupp,³ especially in view of the fact that closely related triplet biradicals are known to give the thermodynamically favored [4 + 2]-adducts.^{11,12} The concerted thermal 1,3-sigmatropic shift that is favored by Kaupp³ for the rearrangement of [4 + 4] to [4 + 2] adducts is formally the forbidden (cf., however, subjacent orbital control⁴⁰) suprafacial migration with retention at the migrating center.⁶

Experimental Section

Materials. Sources and purification procedures of all compounds used in this work were described previously.^{4c,12,13}

Fluorescence Measurements. A Perkin-Elmer Hitachi MPF-2A spectrophotometer was employed. Temperature control, temperature monitoring, and sample preparation were as previously described.¹³ Lifetime measurements were performed at room temperature under degassed and air-saturated conditions on a SLM 4800C phase-modulation spectrofluorimeter. The excitation light was passed through a monochromator and was then intensity modulated in an ethanol/water mixture (19:81, v/v) at 30 MHz. A solution of glycogen in water was

(38) Masnovi, J. M.; Kochi, J. K.; Hilinski, E. F.; Rentzepis, P. M. *J. Am. Chem. Soc.* **1986**, *108*, 1126-1135.

(39) Eckert, G.; Goetz, M. *J. Am. Chem. Soc.* **1994**, *116*, 11999-12009.

(40) Berson, J. A.; Salem, L. *J. Am. Chem. Soc.* **1972**, *94*, 8917-8918.

used as a scatterer for the reference. The emission intensities of the sample and scattering solutions were closely matched for each measurement using neutral density filters. The phase shift and modulation of each sample were measured 10 times and the results averaged. Reported lifetimes are averages of 10 independent measurements.

Picosecond Laser Spectroscopy. The modified Quantel/Continuum Nd:YAG laser system used to record the transient absorption spectra was described previously.⁴¹ Briefly, it consists of an actively-passively mode-locked Nd:YAG oscillator and a double-pass Nd:YAG amplifier. Excitation pulses exhibiting a half-width of ~25 ps at 355 nm were generated from the 1064-nm fundamental by means of a third-harmonic generating crystal. The energies of the excitation pulses were measured by diverting ~10% of each pulse into the probe (Model RjP-735) of an energy meter (Laser Precision Corp. Model Rj-7200) and were in the range of 0.1–0.2 mJ/pulse. The energies of the excitation laser pulses were in the range for which the signal intensity depends linearly on pulse energy. The beam diameter at the sample was ~2 mm.

The absorbance change at a selected time after excitation was monitored by means of a 30-ps continuum pulse. This white-light probe pulse was generated when the sufficiently energetic portion of the split, original 1064-nm pulse was focused into a 20-cm cell that contained a 1:1 H₂O/D₂O mixture. The probe pulse was split and directed into the sample cell and the reference cell. After transmission through these cells, the probe pulses were focused at the slit of a 0.32-m spectrograph (Instruments SA Model HR-320). The spectrograph output was imaged onto an EG&G Princeton Applied Research (PAR) two-dimensional silicon intensified target detector (Model 1254E) coupled to a PAR 1216 multichannel detector controller. This detector was interfaced with an IBM microcomputer that controlled the necessary optical

hardware and electronics during data acquisition, processed the data, and presented the data graphically.

To improve the signal-to-noise ratio, each difference absorption spectrum is the result of averaging data from at least 400 excitation laser pulses. A difference absorption spectrum spanning a wavelength range from ~425 to 790-nm is the result of splicing two spectra recorded in the 425–640-nm and the 555–790-nm regions at a selected time after excitation. For the 425–640-nm region, most of the fluorescence from ¹DCA* has been subtracted. The fluorescence is more noticeable at early times for wavelengths <525 nm. To acquire data for each transient absorption spectrum, the sample was flowed through a 2-mm pathlength fused silica flow cell at a rate sufficient to replace the volume that was exposed to the excitation pulses impinging on the sample at a rate of 10 pulses/s. The sample solution was bubbled with a stream of argon prior to an experiment and maintained under argon during an experiment.

Irradiation Procedures, Light Filters, and Lamps. Preparative and quantum yield irradiations were carried out as previously described.¹³

Analyses. Instruments used in absorption measurements, UV and NMR, and for gas-liquid chromatography were also described previously.¹³

Acknowledgment. Work at Florida State University was supported by NSF, most recently by Grant No. CHE 93-12918. R. Dabestani acknowledges support from the Division of Chemical Sciences, Office of Basic Energy Sciences, U.S. Department of Energy under contract No. DE-AC0584OR21400 with Martin Marietta Energy Systems Inc. We thank Professor R. A. Caldwell for helpful discussions.

JA9507877

(41) Schmidt, J. A.; Hilinski, E. F. *Rev. Sci. Instrum.* **1989**, *60*, 2902–2914.